

AIB-VINCOTTE



FOREST CENTRAL OFFICE

Avenue du Roi, 157 - B-1060 Brussels
Phone (2) 536 82 11 - Telex 22550 - Fax (2) 537 46 19

Report n°47-3-0052-4

June, 1994

**THE PISC PARAMETRIC STUDY ON THE EFFECT OF
THE TEXTURE OF CAST AUSTENITIC STAINLESS STEEL**

ASME Pressure Vessel and Piping Conference

Minneapolis, USA, June 1994

G. MAES, B. HANSOUL, Ph. DOMBRET

THE PISC PARAMETRIC STUDY ON THE EFFECT OF THE TEXTURE OF CAST AUSTENITIC STAINLESS STEEL

Guy Maes, Brigitte Hansoul, Philippe Dombret
R&D Department
AIB-Vinçotte
Brussels
Belgium

ABSTRACT

Within the framework of Action 4 (Austenitic Steel Testing) of PISC III, a parametric study was carried out on a set of centrifugally cast stainless steel samples, representative of the main coolant piping of pressurized water nuclear reactors. The samples are obtained from different manufacturers, and feature various grain textures and dimensions.

Artificial and realistic flaws were used to assess the detection and sizing capability of ultrasonic examination techniques. The paper analyzes the data as a function of the metal structure and of the main parameters of the testing techniques, which include TRL contact probes and immersion focusing transducers.

Guidelines are deduced as to the selection of inspection techniques, in relation with the metallurgical texture of each specimen. In addition, the influence of the presence of a weld across the wavepath is evaluated, as well as the similarity between the responses obtained from crack-like machined reflectors and mechanical fatigue cracks.

1. INTRODUCTION

The various Actions that constitute PISC III (1) have each their specific scope and programme. Action 4 aims at assessing the inspection capability of non-destructive evaluation (NDE) techniques and procedures in austenitic stainless steel components, such as the main coolant piping and the auxiliary piping of light water nuclear reactors (2).

That objective leads to consider cast and wrought base materials, as well as weld joints. The manufacturing processes involved can produce very different grain textures, which hardly lend themselves to NDE; castings and welds are recognized as the worst cases as a result of their coarse-grain textures (3).

PISC Action 4 started capability studies, for different material types, as round-robin tests. In addition, parametric studies were decided to assess the effect of specific parameters on the

inspection results. This paper describes a study performed on centrifugally cast austenitic steel samples to evaluate the influence of various metallurgical textures of coarse-grain materials.

2. MEASUREMENT PROCEDURE

2.1. Steel Specimens

Six centrifugally cast steel blocks, with various material structures, were made available by the PISC programme; typical macrographs are shown in Figure 1. All specimens are sectors of piping with outside diameters ranging from 803 mm to 905 mm, and a wall thickness of approximately 60 mm. They are representative of the main coolant piping of pressurized water nuclear reactors.

Table 1 provides further details on the specimens and on their reflectors. Two blocks contain a weld, with a crack propagated in the heat-affected zone by mechanical fatigue. In the other four, a 6 mm deep circular slot was machined, beside conventional ASME-type reflectors. That slot is identical to the smooth and sharp defects commonly used in PISC, and referred to as type-A flaws.

In addition, a carbon steel block, with the same geometry, was provided as a reference specimen, and for probe characterization purposes.

2.2. Equipment

Automated ultrasonic examination of the specimens was performed using motorized scanning devices and a computerized data acquisition system. The associated software code enables the operator to control the equipment, as

well as to store, visualize and process the ultrasonic data.

A set of 45° probes is listed in Table 2, with their nominal characteristics measured on the carbon steel reference block. They were selected, on the basis of preliminary manual investigations, to assess the influence of the search unit parameters on the testing capability. They include a 1 MHz shear wave transducer and 4 twin-crystal compression wave (TRL) probes with various frequencies and depth ranges. It should be noted that the model referred to as V3309 corresponds to the most commonly used technique for PWR main coolant piping inspection.

Additionally, a large (100 mm emitter dia.) immersion focusing probe, also generating compression waves at 45° in steel, was considered to illustrate the potential of one exemplative advanced technique.

2.3. Data Acquisition

The examination of the pipe sections was conducted from the outside surface, scanning parallel to the pipe axis. Scanning steps and increments of 1 mm allowed for accurate amplitude measuring and reflector imaging.

A flaw is considered detected, if the peak echo amplitude exceeds the noise level at the same depth range. The noise level is estimated, on the graphical data display, as the amplitude of the highest noise peaks that are likely to disturb reliable contouring of a flaw indication. The precision of this graphical method is roughly evaluated at 2 dB. Moreover, it must be realized that noise level variations of several dB can be encountered at constant depth in any specimen.

Both maximum amplitude and signal-to-noise ratio (SNR) are determined for each reflector. Unless stated otherwise, the amplitude values used in the following are relative figures, with regard to the same reflector in the carbon steel reference specimen.

3. DATA EXPLOITATION

3.1. Influence of Weld Material

The presence of a crack in the heat-affected zone of 2 specimens (Fig. 1d) allows to assess the influence of the weld texture and of the interfacing fusion lines in the ultrasonic wavepath.

Insonifying the flaws from both sides successively yields contradictory conclusions: whereas, for the TRL probes, the corner echoes reflected by the cracks are generally higher when crossing the weld, the contrary holds for the focusing transducer. However, the observed differences never exceed 3 dB. Similarly, no significant effect can be inferred from the signal-to-noise ratio data. Figure 2 summarizes the measurements on the 22 mm deep crack. Moreover, no flaw mislocations, attributable to beam skewing phenomena, was assessed.

As a consequence, it can be concluded that the welds of the 2 specimens considered do not disturb the propagation of compression waves.

3.2. Flaw Detection Capability of Probes

The overall detection capability of each probe can be deduced from the averaged data given in Figure 3, which takes into account all reflectors in the weldless austenitic specimens. For the 1 MHz shear wave probe, no values are reported, since no reflector in any of the specimens was detected. This only confirms the generally poor performance of shear vertical wave transducers in cast austenitic textures, which has been demonstrated experimentally and by numerical simulations.

All compression wave probes show a loss of echo amplitude of at least 5 dB, with regard to the carbon steel reference, except for the low frequency (0.5 MHz) V3325P TRL probe. In addition, this transducer is only slightly disturbed by the grain structure, and it offers an average signal-to-noise ratio of 8 dB over the depth range from 15 to 60 mm.

Figure 4 illustrates the limitations of the 2 MHz (V3534) transducer on deep reflectors. This is partly due to its geometrical design, but the major cause lies in the influence of the austenitic material texture on the propagation of too high frequency sound waves. Table 3 displays the shift of the probe signal frequency, with reference to carbon steel, measured on side-drilled holes in the stainless steel test specimens. Clearly, coarse-grain austenitic materials act as a low-pass filter on the ultrasonic waveform, thereby reducing considerably the actual sensitivity of transducers working above 1 MHz.

Figure 4 also compares the 1 MHz TRL probes: whereas the conventional V3309 transducer cannot detect the sharp slots machined in the mixed textures of blocks 21 and 22, the V3326R, which is based on larger piezoelectric elements for an increased depth range, succeeds in all specimens, and collects an average signal-to-noise ratio about 5 dB higher than the former probe. The example given in Figure 5 illustrates additionally the resolution of the images, and the absence of flaw tip echoes.

Similarly, Figure 6 compares images obtained with the V3326R TRL transducer and with the focused beam probe on the 22 mm high crack of specimen W455-D. It highlights the improvement provided by the concentration of sound energy in the focal zone (4), with the same frequency, refracted angle, and scan direction. The superior performance of the beam focusing technique is corroborated by measurements carried out on side-drilled holes and slots: Figure 4 shows signal-to-noise ratio improvements of about 6 dB, with regard to the best TRL search units.

3.3. Influence of Base Material Texture

Figure 7 displays the average signal-to-noise ratio calculated, for all specimens, from measuring each reflector with each probe. A ranking of the different steel structures appears, in terms of ultrasonic inspectability. The mixed coarse-grain texture of specimens 21 and 22 turns out to be the most difficult to inspect, while the columnar grains of specimen 25 obviously cause less trouble.

Table 4 quantifies the signal-to-noise ratio variation to be expected in inspection practice between so-called difficult and easy austenitic steel structures. On the basis of measurements achieved with two probes well-suited for such tasks, a difference of typically 10 dB is assessed at full depth.

The materials considered can also be classified according to their low-pass filtering effect: Table 3 shows results of the analysis, in the frequency domain, of the waveforms reflected by side-drilled holes. This leads to a very similar ranking, except for the equiaxed texture of specimen 24, which produces a larger centre frequency shift, in spite of its smaller grain dimension.

Indeed, most probes considered allow for reliable detection in the dendritic structure of specimen 25. This confirms both theoretical and experimental studies on austenitic material structures (5), showing that acoustic propagation is only slightly affected when the angle between the ultrasonic beam axis and the dendrite orientation is approximately 45°.

3.4. Comparison Between Machined Slot and Fatigue Crack

Machined slots similar to those of specimens 21 to 25 have been extensively used in PISC to simulate smooth cracks realistically. Whereas the validity of the approach has been thoroughly verified for shear wave insonification, few data exist for the case of compression waves in austenitic materials. The availability of a 10 mm high mechanical fatigue crack, in specimen W455-D, and of 6 mm high slots in the weldless specimens, provided the opportunity of a useful, though very limited, comparison.

Figure 8 represents the outcome of the measurements, after amplitude data processing to compensate for the different materials scattering. The detection probabilities of both reflectors appear quite alike. This supports the representativity of the considered slots, with regard to real service-induced cracks.

3.5. Flaw Sizing Capability

If the tip signal of a crack-like reflector is detected and clearly resolved, accurate sizing in height can be achieved between the tip echo and the corner reflection. Due to its enhanced signal-to-noise ratio and lateral resolution, the focusing transducer allows for detecting and resolving crack tip signals in some of the considered steel structures. Figure 9 shows the ultrasonic imaging of a slot which was accurately sized with the tip diffraction method.

No tip echoes are observed with the TRL probes. Consequently, sizing must typically rely on amplitude-based methods, even though the intrinsic inaccuracy of those is increased by the poor resolution of such low-frequency transducers. As an example, Figure 10 displays images obtained with the 0.5 MHz V3325P probe on 4.8 mm dia. side-drilled holes: the beam width of about 25 mm leads to flagrant oversizing.

4. CONCLUSIONS

Due to the nature of austenitic materials, caution must be taken in transposing results obtained in a specific configuration. Nevertheless, the major observations to be drawn from the study can be summarized as follows:

- As a general rule, shear vertical wave transducers are not suited for the inspection of centrifugally cast austenitic

stainless steel structures.

- The adverse effects of material textures increase with the wall thickness to be inspected, and with the sound wave frequency.
- 0.5 MHz compression waves propagate properly, but lead to insufficient resolution for good sizing; 2 MHz waves, on the contrary, come up against the strong scattering caused by the grains. As a rule, 1 MHz appears to be the most effective frequency in the available specimens.
- The measurements highlighted the severe limitations of the flaw detection and sizing capability of the TRL probe that corresponds to the usual examination practice in industry; alternative TRL designs were proved more effective in the far-surface region.
- The acoustic beam focusing technique was shown to provide a higher capability than TRL transducers, for flaw detection and sizing.
- The examination of the columnar grain texture appears to be the easiest one; that conclusion must however be tempered by the fact that the 45° angle used between the wave direction and the dendrite orientation favours the acoustic propagation.
- Considering the flaw detection capability, the mixed textures led to the lowest signal-to-noise ratios; on the other hand, the equiaxed grains appeared to shift significantly the pulse frequency of the various transducers.
- No obvious influence of the weld could be observed in the measurements carried out.
- An experimental contribution to the demonstration of the representativeness of sharp artificial slots, with regard to service-induced cracks, was provided.
- As tip echoes can hardly be distinguished, the planar flaw sizing capability is rather poor.

ACKNOWLEDGEMENTS

This work was performed with a financial support of the Joint Research Centre Ispra of the Commission of the European Communities.

REFERENCES

1. S. Crutzen, R. Nichols, A. G. Miller, "PISC III : A Status Report", ASME PVP Conference, Denver (CO), July 1993
2. S. R. Doctor, P. Lemaître, C. Vinche, "Austenitic Steel Piping Testing Exercises in PISC", SMIRT 12 Post-Conference Seminar n°2, Paris (F), August 1993
3. Handbook on the Ultrasonic Examination of Austenitic Welds, International Institute of Welding, edited by the American Welding Society, 1985
4. G. Maes, M. Delaide, Ph. Dombret, "On the Use of the Ultrasonic Beam Focusing Technique", 11th Int. Conference on NDE in the Nuclear and Pressure Vessel Industry, Albuquerque (NM), 1991
5. M. G. Silk, "Ultrasonic Techniques for Inspecting Austenitic Welds", in Research Techniques in NDT, Vol. IV, Academic Press, 1980

SPECIMEN	MATERIAL	REFLECTORS
21	CCSS, mixed structure	side-drilled holes ($\varnothing = 4.8$ mm), machined slot (h = 6 mm), milled notch (1.2 x 4 mm)
22	CCSS, mixed structure	side-drilled holes ($\varnothing = 4.8$ mm), machined slot (h = 6 mm), milled notch (1.2 x 4 mm)
24	CCSS, equiaxed structure	side-drilled holes ($\varnothing = 4.8$ mm), machined slot (h = 6 mm)
25	CCSS, columnar structure	side-drilled holes ($\varnothing = 4.8$ mm), machined slot (h = 6 mm)
W455-D	CCSS, equiaxed, welded	side-drilled holes ($\varnothing = 4.8$ mm), fatigue crack (h=22 mm)
W455-E	CCSS, equiaxed, welded	fatigue crack (h=10 mm)
29	Carbon steel	side-drilled holes ($\varnothing = 4.8$ mm), machined slot (h = 6 mm), milled notch (1.2 x 4 mm)

TABLE 1 : TEST SPECIMENS AND REFLECTORS

PROBE	WAVE TYPE	PROBE TYPE	COUPLING	HOUSING WxLxH	FREQUENCY	-6 dB DEPTH RANGE
V3325P	Compression	TRL	Contact	60x60x45 mm	0.5 MHz	10 - 135 mm
V3309	Compression	TRL	Contact	50x40x38 mm	1 MHz	20 - 110 mm
V3326R	Compression	TRL	Contact	60x60x45 mm	1 MHz	25 - 135 mm
V3534	Compression	TRL	Contact	30x30x31 mm	2 MHz	10 - 45 mm
WB45-1E	Shear	Single cryst.	Contact	32x55x50 mm	1 MHz	
IF-100	Compression	Focused	Immersion	\varnothing 110x50 mm	1 MHz	20 - 75 mm

TABLE 2 : UT TRANSDUCERS (ALL 45° REFRACTED);
(NOTE : CHARACTERISTICS ARE MEASURED IN CARBON STEEL)

PROBE SPECIMEN	V3325P (0.5 MHz)	V3309 (1 MHz)	V3326R (1 MHz)	V3534 (1 MHz)	SPECIMEN AVG
21	-0.03	-0.10	-0.09	-0.60	-0.21
22	-0.08	-0.02	-0.09	-0.63	-0.21
24	-0.03	-0.13	-0.18	-0.70	-0.26
25	-0.06	-0.11	-0.13	-0.28	-0.15
PROBE AVG	-0.05	-0.09	-0.12	-0.55	(MHz)

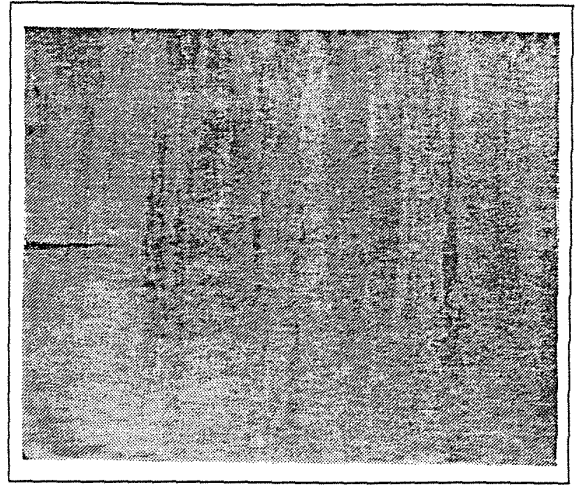
TABLE 3 : SIGNAL FREQUENCY SHIFT (IN MHZ) WITH REFERENCE TO CARBON STEEL
(NOTE : ALL MEASUREMENTS ON 4.8 MM DIAMETER SIDE-DRILLED HOLES)

	MIXED COARSE GRAIN		COLUMNAR		DIFFERENCE	
	V3309	V3326R	V3309	V3326R	V3309	V3326R
SDH at 45 mm	8	10	16	21	8	11
SLOT	0	1	8	14	8	13

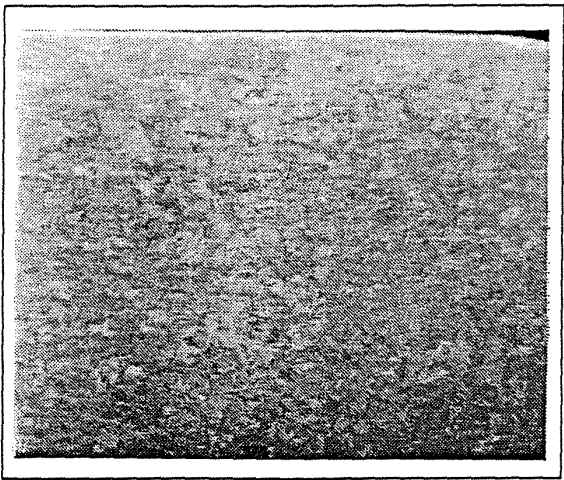
TABLE 4 : SIGNAL-TO-NOISE RATIO VALUES (IN DB) OBTAINED WITH 1 MHZ TRL PROBES,
IN TWO DIFFERENT TEXTURES



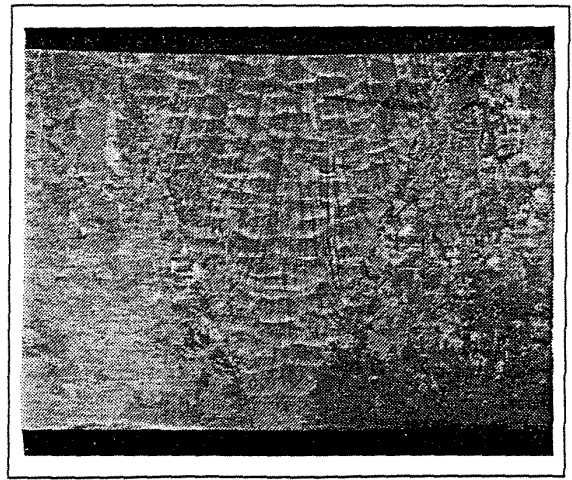
A) MIXED COARSE-GRAIN STRUCTURE (21)



B) COLUMNAR STRUCTURE (25)



C) EQUIAXED STRUCTURE (24)



D) WELDED SPECIMEN (W455-D)

FIG. 1. GRAIN STRUCTURE OF SPECIMENS

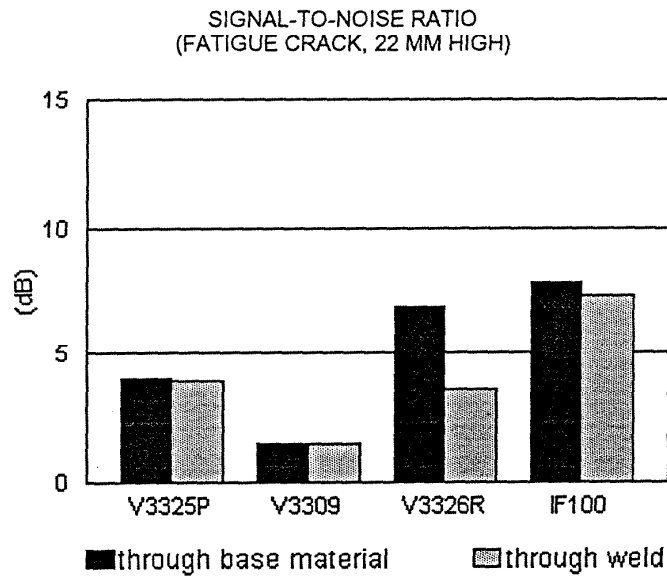
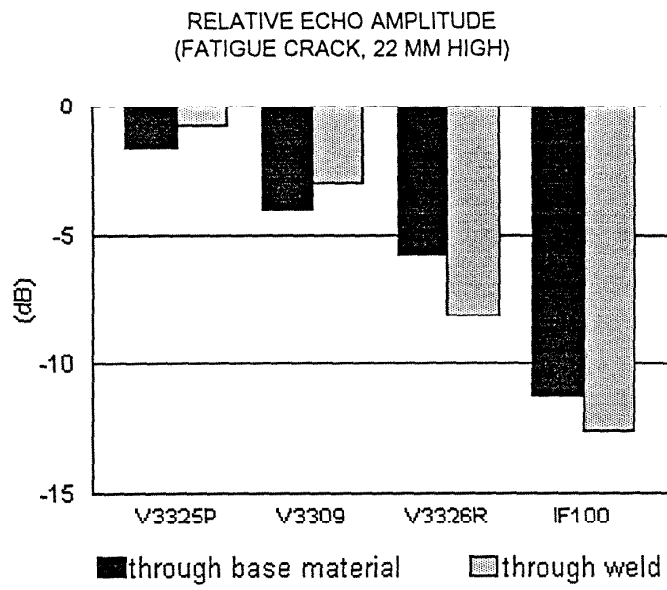


FIG. 2. AMPLITUDE (TOP) AND SIGNAL-TO-NOISE RATIO (BOTTOM) OF CORNER REFLECTIONS FROM THE FATIGUE CRACK IN SPECIMEN W455-D

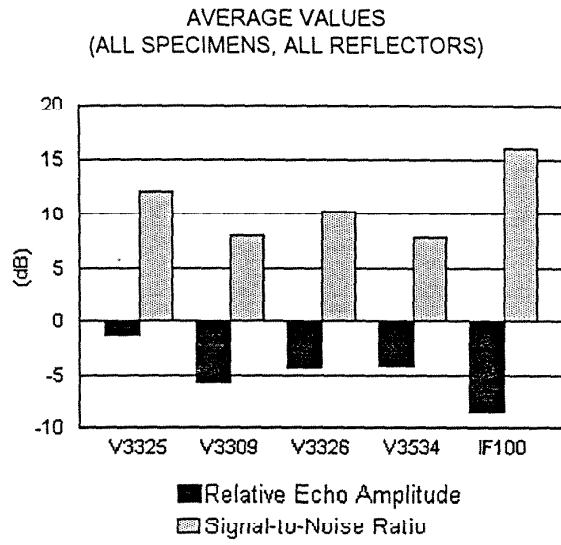


FIG. 3. AVERAGE ECHO AMPLITUDE AND SIGNAL-TO-NOISE RATIO IN WELDLESS SPECIMENS

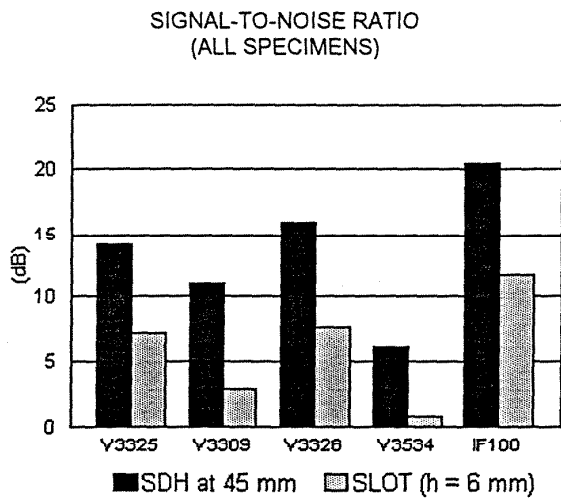


FIG.4. DETECTION PERFORMANCE ON ARTIFICIAL REFLECTORS NEAR TO THE FAR SURFACE

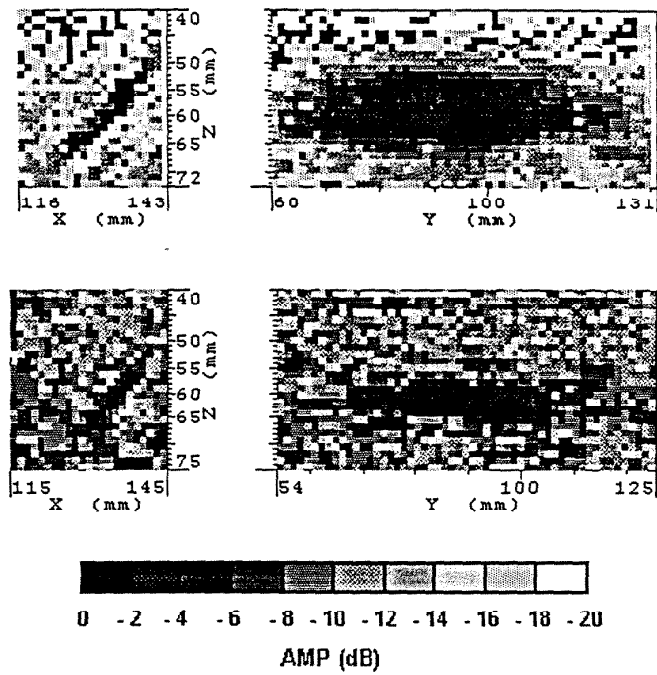


FIG. 5. B-SCAN (LEFT) AND D-SCAN (RIGHT) VIEWS OF A 6 MM HIGH SLOT IN SPECIMEN 25; V3326R TRANSDUCER (TOP) AND V3309 TRANSDUCER (BOTTOM)

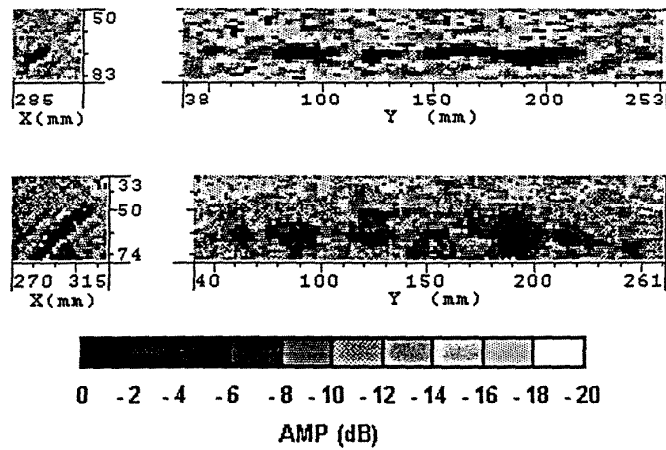


FIG.6. B-SCAN (LEFT) AND D-SCAN (RIGHT) VIEWS OF A 22 MM HIGH MECHANICAL FATIGUE CRACK IN SPECIMEN W455-D; 1 MHZ FOCUSED BEAM PROBE (TOP) AND V3326R TRANSDUCER (BOTTOM)

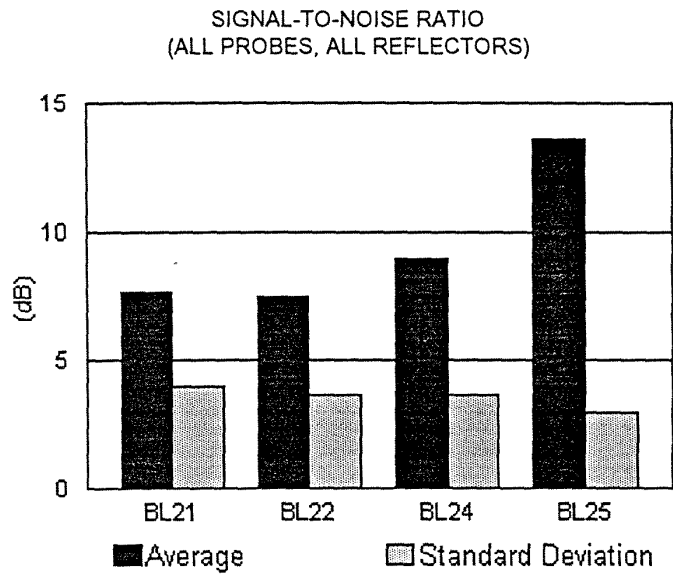


FIG.7. INFLUENCE OF MATERIAL STRUCTURE

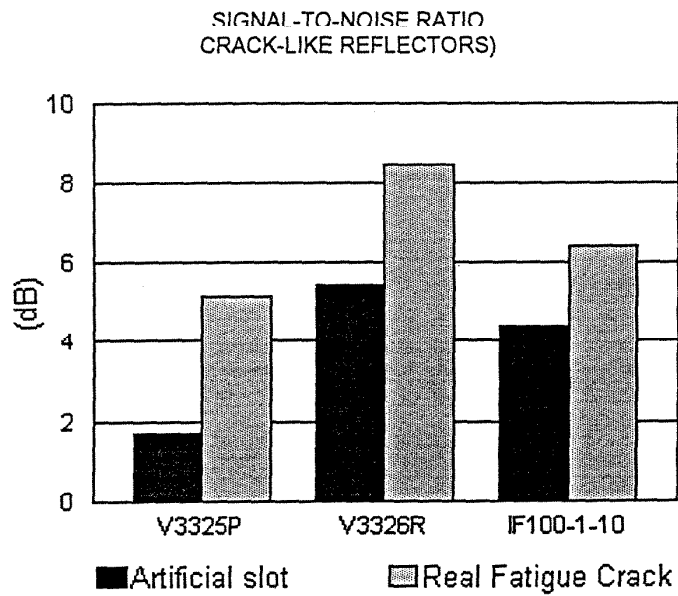


FIG.8. SIGNAL-TO-NOISE RATIO OF CORNER ECHO REFLECTED BY A FATIGUE CRACK (H = 10 MM) AND A MACHINED SLOT (H = 6 MM)

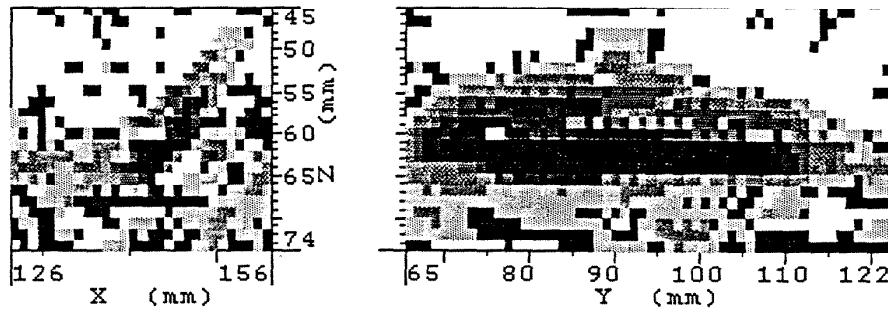


FIG. 9. B-SCAN (LEFT) AND D-SCAN (RIGHT) VIEWS OF A 6 MM HIGH SLOT IN SPECIMEN 25, OBTAINED WITH 1 MHZ COMPRESSION WAVE FOCUSING TRANSDUCER (BEAM DIAMETER 9 MM)

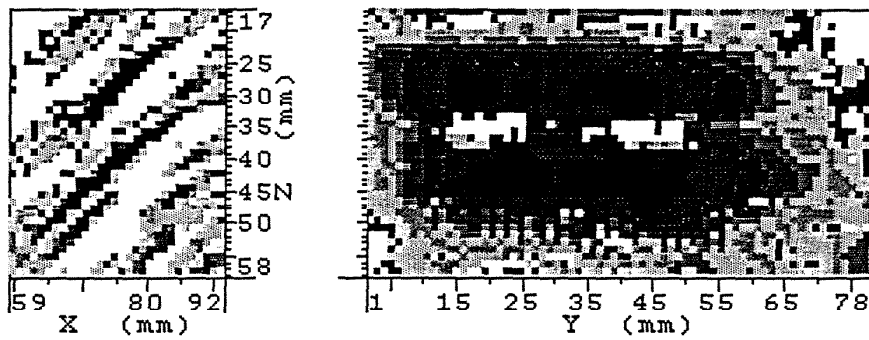


FIG. 10. B-SCAN (LEFT) AND D-SCAN (RIGHT) VIEWS OF 4.8 MM DIAMETER SIDE-DRILLED HOLES IN SPECIMEN 25, OBTAINED WITH 0.5 MHZ V3325P TRANSDUCER (BEAM DIMENSION 25 TO 30 MM)